Clinical and Experimental Obstetrics & Gynecology

Clin. Exp. Obstet. Gynecol. **2026**; 53(2): 46979
https://doi.org/10.31083/CEOG46979

Original Research

Clinical and Ultrasonographic Features of Uterine Inflammatory Myofibroblastic Tumor: A Six-Case Series

Yutian Miao[1,2], Menghan Liu[1,2], Ke Yang[1,2], Xiao Duan[3], Haiyan Kuang[1,2], Yingchun Luo[1,2], Yu Long[1,2,*]

[1]NHC Key Laboratory of Birth Defect for Research and Prevention, Hunan Provincial Maternal and Child Health Care Hospital, 410008 Changsha, Hunan, China
[2]Ultrasound Medical Center, Hunan Provincial Maternal and Child Health Care Hospital, 410008 Changsha, Hunan, China
[3]Department of Radiology, 921st Hospital of the Joint Logistic Support Force of the Chinese People's Liberation Army, 410003 Changsha, Hunan, China
*Correspondence: 362714407@qq.com (Yu Long)
Academic Editor: Michael H. Dahan
Submitted: 28 September 2025 Revised: 12 November 2025 Accepted: 28 November 2025 Published: 10 February 2026

Abstract

Background: This study aimed to analyze the clinical and ultrasonographic features of 6 pathologically confirmed cases of uterine inflammatory myofibroblastic tumors (UIMT) and to enhance clinicians' ability to achieve timely diagnosis and treatment. **Methods**: This retrospective case series included 6 patients with pathologically confirmed UIMT who were admitted to our hospital between January 2019 and January 2025. Clinical, ultrasonographic, and pathological data were collected and analyzed retrospectively. **Results**: All 6 tumors were solid and originated from the myometrium. 3 were confined to the myometrium, 2 extended toward the submucosa, and 1 toward the subserosa. 5 lesions were hypoechoic and 1 was hyperechoic, all showing heterogeneous internal echoes and a characteristic "blurred halo sign". The median maximum diameter was 6.9 cm. Color Doppler flow imaging (CDFI) showed an Adler grade $\geq$2, demonstrating a "colorful mosaic sign". During follow-up, 2 lesions increased in size by 1 cm and 2 cm, respectively, within 2–4 months. No extrauterine metastasis was observed. All cases were positive for anaplastic lymphoma kinase (*ALK*), as confirmed by fluorescence in situ hybridization (FISH). All patients underwent surgical treatment, including 1 total hysterectomy and 5 local resections. No recurrence or metastasis was observed during 21–57 months of follow-up. **Conclusions**: UIMT exhibits characteristic sonographic features, including solid masses with heterogeneous internal echoes ("blurred halo sign") and abundant blood flow signals ("colorful mosaic sign"). Recognizing these distinctive imaging patterns is critical for improving diagnostic accuracy and guiding appropriate clinical management.

Keywords: uterine inflammatory myofibroblastic tumor; ultrasonography; blurred halo sign; colorful mosaic sign; diagnosis

1. Introduction

Inflammatory myofibroblastic tumor (IMT) is a rare neoplasm characterized by the proliferation of myofibroblastic spindle cells accompanied by marked inflammatory infiltration [1]. It mainly occurs in the lungs and soft tissues of the abdomen, while uterine involvement is uncommon. This etiology remains uncertain but may be associated with chronic infection, autoimmune disorders, or trauma [2]. According to the latest World Health Organization (WHO) classification, approximately 5% of IMT cases may recur or metastasize [3]. Because of its morphological similarity to other spindle cell tumors of the female reproductive tract, uterine IMT (UIMT) is often misdiagnosed as a smooth muscle tumor. Studies on the ultrasonographic manifestations of UIMT are limited and mostly confined to isolated case reports. Therefore, this study systematically analyzes UIMT's clinical and ultrasonographic characteristics to enhance clinicians' understanding and facilitate timely diagnosis and treatment.

2. Materials and Methods

2.1 Instruments and Methods

This was a retrospective case analysis including 6 UIMT patients confirmed by surgery and pathology at our hospital between January 2019 and January 2025. Inclusion criteria: Postoperative pathological findings consistent with the diagnostic criteria for UIMT in the [2020 WHO Classification of Soft Tissue and Bone Tumours] [1], characterized by spindle cell proliferation with inflammatory cell infiltration and positive anaplastic lymphoma kinase (*ALK*) expression; complete preoperative transvaginal three-dimensional (3D) ultrasonography data and clinical medical records. Exclusion criteria: Concurrent gynecological malignancies or other soft tissue tumors; incomplete ultrasonographic data; loss to follow-up. Ultrasonographic examinations were performed using GE E8, GE E6 (General Electric Company, Waukesha, WI, USA), and Philips IU22 systems (Philips Healthcare, Best, North Brabant, the Netherlands) equipped with transvaginal 3D probes (4–9 MHz). All scans were conducted by obstetric and gynecologic ultrasound physicians with more than 10 years of ex-

perience. Clinical data, including demographic characteristics and diagnosis/treatment information, were retrieved from the hospital's electronic medical records system. Ultrasonographic data were extracted from the imaging reporting system, documenting lesion mass characteristics such as location, size, shape, margin, internal echo pattern, and blood flow signals. Blood flow was assessed using the Adler semi-quantitative grading system [4]: Grade 0 (no detectable flow); Grade 1 (scant flow, 1–2 punctate/short rod-like signals); Grade 2 (moderate flow, 3–4 punctate/short rod-like signals or a vessel diameter $\geq$ mass radius); Grade 3 (abundant flow, >4 vessels or interconnected network). Two independent sonographers evaluated all images to ensure consistency. Patient prognosis was assessed through outpatient follow-up and telephone interviews. No recurrence or metastasis was observed in any patients during the follow-up period. The study was approved by the institutional ethics committee (Approval No. JSKY-2025-11-002), informed consent has been obtained from the patient.

2.2 Statistical Analysis

Data analysis was performed using SPSS version 26.0 (IBM Corporation, Armonk, NY, USA). Continuous variables were described as mean $\pm$ standard deviation (SD), median, minimum, and maximum values. Categorical variables were expressed as frequencies (n) and percentages (%).

3. Results

3.1 Clinical Characteristics

A total of 6 patients with pathologically confirmed UIMT were included, aged 24–49 years (mean 37.8 $\pm$ 8.5 years). The main presenting complaint was prolonged menstruation in four patients (66.7%), three of whom also reported increased menstrual volume. Two patients (33.3%) were asymptomatic, with lesions incidentally detected during routine examinations. Among all patients, 3 (50%) experienced dysmenorrhea, 4 (66.7%) had a history of childbirth, 1 had a history of one induced abortion, and 1 was unmarried and nulliparous. All patients (100%) presented with anemia. Elevated white blood cell counts were observed in 3 cases (50%) (11.4×10^9/L, 12.7×10^9/L, and 10.7×10^9/L), while 2 patients (33.3%) had increased cancer antigen 125 (CA125) levels (38.4 U/mL, and 162 U/mL). Additionally, 2 patients (33.3%) had a history of thyroid disease—one with hyperthyroidism and the other with papillary thyroid carcinoma (status post subtotal thyroidectomy). None of the patients was pregnant at diagnosis (See Table 1).

3.2 Ultrasonographic Features

All 6 UIMT cases (100%) underwent ultrasonography, with imaging features summarized in Table 2. All lesions were solid and originated in the myometrium. Three (50%) were confined to the myometrium, 2 (33.3%) protruded toward the submucosa, and 1 (16.7%) extended toward the subserosa. Sonographically, 5 lesions (83.3%) were hypoechoic and 1 was hyperechoic, all demonstrating heterogeneous internal echoes and a characteristic "blurred halo sign"—manifested as scattered strip or patchy slightly hyperechoic areas within a hypoechoic background. Five tumors (83.3%) were oval, and 1 was elongated, with maximum diameters ranging from 4.3 to 9.3 cm (median 6.9 cm). Four (66.7%) had well-defined margins, and 2 (33.3%) had poorly defined boundaries.

According to the Adler classification [4] of color Doppler flow, 4 lesions (66.7%) were Grade 2 and 2 (33.3%) were Grade 3, showing a "colorful mosaic sign". Two patients underwent a single ultrasound examination, while 4 underwent repeat scans. Among the 4 patients who had follow-up ultrasounds, 2 showed no change in tumor size, 1 exhibited a 1 cm increase after 2 months, and another showed a 2 cm increase after 4 months. All lesions were confined to the uterine corpus, with no evidence of extrauterine metastasis.

3.3 Pathological Features

Grossly, the tumors appeared grayish-white to grayish-red with a moderately firm to slightly soft texture, occasionally showing mucoid changes. Among the 6 cases, 2 had well-circumscribed margins, 2 exhibited infiltrative growth, and 2 had poorly defined boundaries. Histologically, 4 (66.7%) cases were classified as the myxoid type, characterized by sparsely arranged spindle or short spindle cells within a myxoid stroma and moderate inflammatory infiltration under low magnification. The remaining 2 cases (33.3%) were dense spindle cell type, composed of compact bundles or fascicles of spindle cells with mild inflammation and focal myxoid changes. High magnification showed mild cellular atypia with abundant, lightly eosinophilic cytoplasm. Immunohistochemistry: All 6 cases (100%) showed *ALK* gene rearrangement confirmed by FISH. Three cases showed partial CD10 positivity, and 2 were H Caldesmon-positive. Estrogen receptor (ER), progesterone receptor (PR), Desmin, smooth muscle actin (SMA), and p16 were positive in all cases. p53 displayed a wild-type expression pattern, and the Ki67 proliferation index ranged from 5% to 30%.

3.4 Treatment and Follow-up Results

All 6 patients underwent surgical treatment. One patient with a submucosal mass received a laparoscopic total hysterectomy. Three patients with intramural masses and 1 patient with a subserosal mass underwent laparoscopic local excision, while 1 patient with a submucosal mass received hysteroscopic electrosurgical resection. The surgical indications included prolonged menorrhagia with anemia, a mass diameter exceeding 5 cm, or rapid mass enlargement within a short period [5]. All patients were preoperatively diagnosed with "uterine space-occupying lesions" based on imaging examinations, and none underwent Tru-cut biopsy

Table 1. Clinical characteristics, treatment, and follow-up of 6 Patients with UIMT.

Number	Age (years)	Clinical Symptoms	Obstetric History (G/P/A)	CA125 (U/mL)	WBC ($\times 10^9$/L)	Hb (g/L)	Surgical Method	Recurrence/Metastasis	Follow-up Time (months)
1	36	Increased menstrual flow, prolonged menstrual period	4/2/2	15.1	9.8	91	Hysteroscopic electroresection of intrauterine neoplasms	no	57
2	38	Uterine mass, dysmenorrhea (detected by physical examination)	1/0/0	38.4	11.4	103	Laparoscopic resection of uterine lesions	no	43
3	49	Increased menstrual flow, prolonged menstrual period	1/1/1	162	12.7	89	Laparoscopic total hysterectomy	no	47
4	39	Increased menstrual flow, prolonged menstrual period, dysmenorrhea	3/1/2	31.9	10.7	83	Laparoscopic resection of uterine lesions	no	26
5	41	Prolonged menstrual period	3/1/2	32.7	6.4	100	Laparoscopic resection of uterine lesions	no	33
6	24	Uterine mass, dysmenorrhea (detected by physical examination)	0/0/0	18.6	5.2	100	Laparoscopic resection of uterine lesions	no	21

Note: G, gravidity; P, parity; A, abortion; WBC, white blood cell; Hb, hemoglobin; CA125, cancer antigen 125; UIMT, uterine inflammatory myofibroblastic tumor.

Table 2. Ultrasonographic features of 6 UIMT cases.

Number	Location	Echogenicity	Echo structure	Shape	Boundary	Solid/cystic	Maximum diameter of the tumor (cm)	Change in tumor size	CDFI (Adler classification)
1	Submucosal	hypoechoic	Heterogeneous echo	elongated	clear	solid	4.3	First detected	2
2*	Intramural	hyperechoic	Heterogeneous echo	oval-shaped	clear	solid	5.7 → 6.7	Increased by 1 cm in two months (↑)	3
3*	Submucosal	hypoechoic	Heterogeneous echo	oval-shaped	clear	solid	3.6 → 5.3	Increased by 2 cm in four months (↑)	3
4	Intramural	hypoechoic	Heterogeneous echo	oval-shaped	poorly defined	solid	7.3	No change within one month	2
5	Subserosal	hypoechoic	Heterogeneous echo	oval-shaped	clear	solid	7.1	First noted	2
6	Intramural	hypoechoic	Heterogeneous echo	oval-shaped	poorly defined	solid	9.3	No change within one month	2

Note: CDFI, color Doppler Flow Imaging; * indicates tumor enlargement.

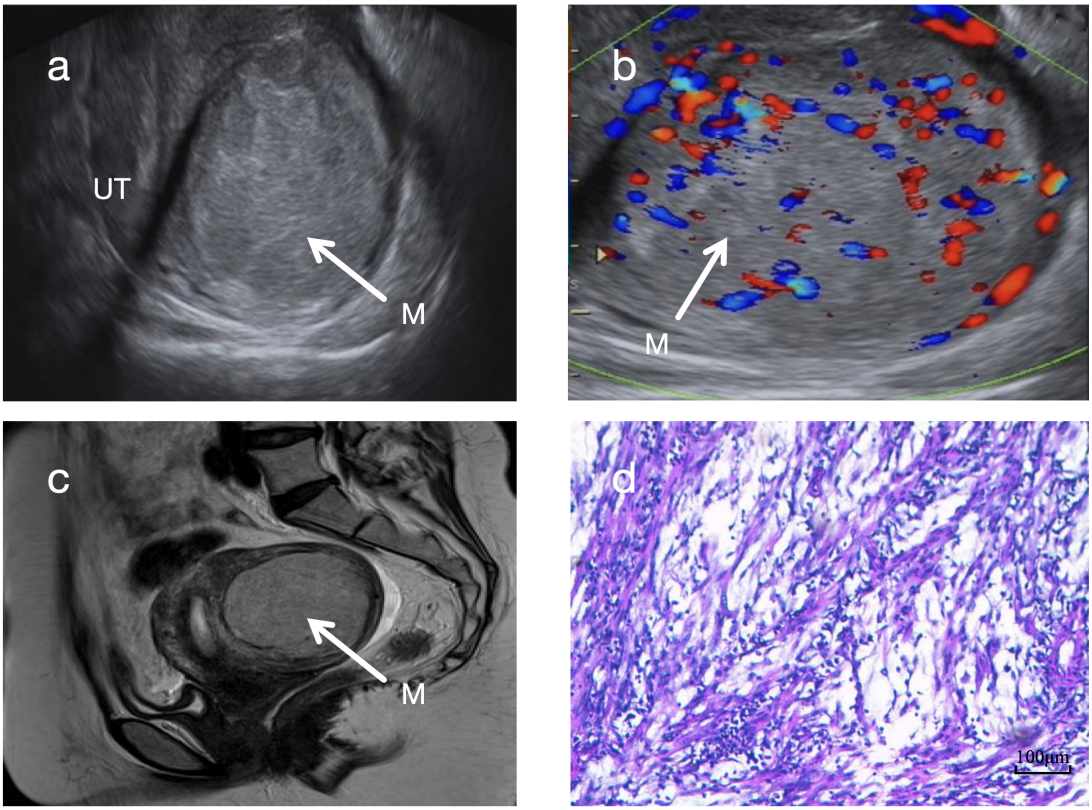

Fig. 1. Ultrasonographic and Pathological Images of Case 2. (a) Sagittal 2D ultrasound image showing a hyperechoic mass in the posterior uterine wall with a "blurred halo sign". (b) Color Doppler ultrasound demonstrating abundant intralesional blood flow signals (Adler grade 3) with a "colorful mosaic sign". (c) T2-weighted MRI revealing a slightly hyperintense mass. (a,b,c) White arrows indicate the tumor masses. (d) HE staining (100×) showing spindle cells with inflammatory cell infiltration (Scale bar = 100 μm). M, mass; 2D, two-dimensional; UT, Uterus; MRI, magnetic resonance imaging; HE, hematoxylin and eosin staining.

before surgery. During the follow-up period of 21–57 months, no cases of recurrence or metastasis were observed.

4. Discussion

4.1 Analysis of Ultrasonographic Features of Uterine Inflammatory Myofibroblastic Tumor

This study demonstrated that UIMT can arise in various locations within the uterine corpus [6,7], consistent with previous findings. In addition, Bhardwaj *et al*. (2025) [8] reported cases involving the cervical region, suggesting that the anatomical distribution of UIMT may be relatively extensive.

In terms of internal echogenicity, UIMT typically presents as hypoechoic, although hyperechoic appearances can also occur. The latter may be associated with increased tumor cell cellularity and pronounced inflammatory cell infiltration (Fig. 1a). Moreover, most UIMT lesions exhibit heterogeneous internal echoes, likely resulting from the irregular interlacing of collagen fibers within the tumor stroma [9].

In this study, all 6 cases of UIMT presented as solid masses, in agreement with the findings of Bai *et al*. (2024) [6]. Therefore, the presence of solid components may be considered a characteristic sonographic feature of UIMT. Zhao *et al*. (2022) [10] described a case of UIMT containing cystic components, possibly arising from inflammatory infiltration, intratumoral hemorrhage, or cystic necrosis.

From the perspective of tumor size and growth characteristics, UIMT masses are often relatively large. The median maximum diameter of UIMT masses in this study was 6.9 cm, slightly larger than the 5 cm reported by Bai *et al*. [6]. Additionally, the color Doppler flow signals in this cohort were more abundant, suggesting that a rich vascular supply may contribute to tumor enlargement. Notably, the masses in Case 2 and Case 3 showed rapid growth over a short period, likely reflecting the biologically active proliferation nature of UIMTs. The combination of "rapid enlargement over a short period and abundant blood flow signals" should be regarded as an important diagnostic alert for UIMT. Recognition of this pattern may prevent clinicians from overlooking potentially borderline tumors that appear morphologically benign. Ultrasonographic evaluation revealed ill-defined margins in Cases 4 and 6, which corresponded pathologically to infiltrative growth into the surrounding smooth muscle. This finding highlights the diagnostic value of evaluating tumor margins during ultrasonog-

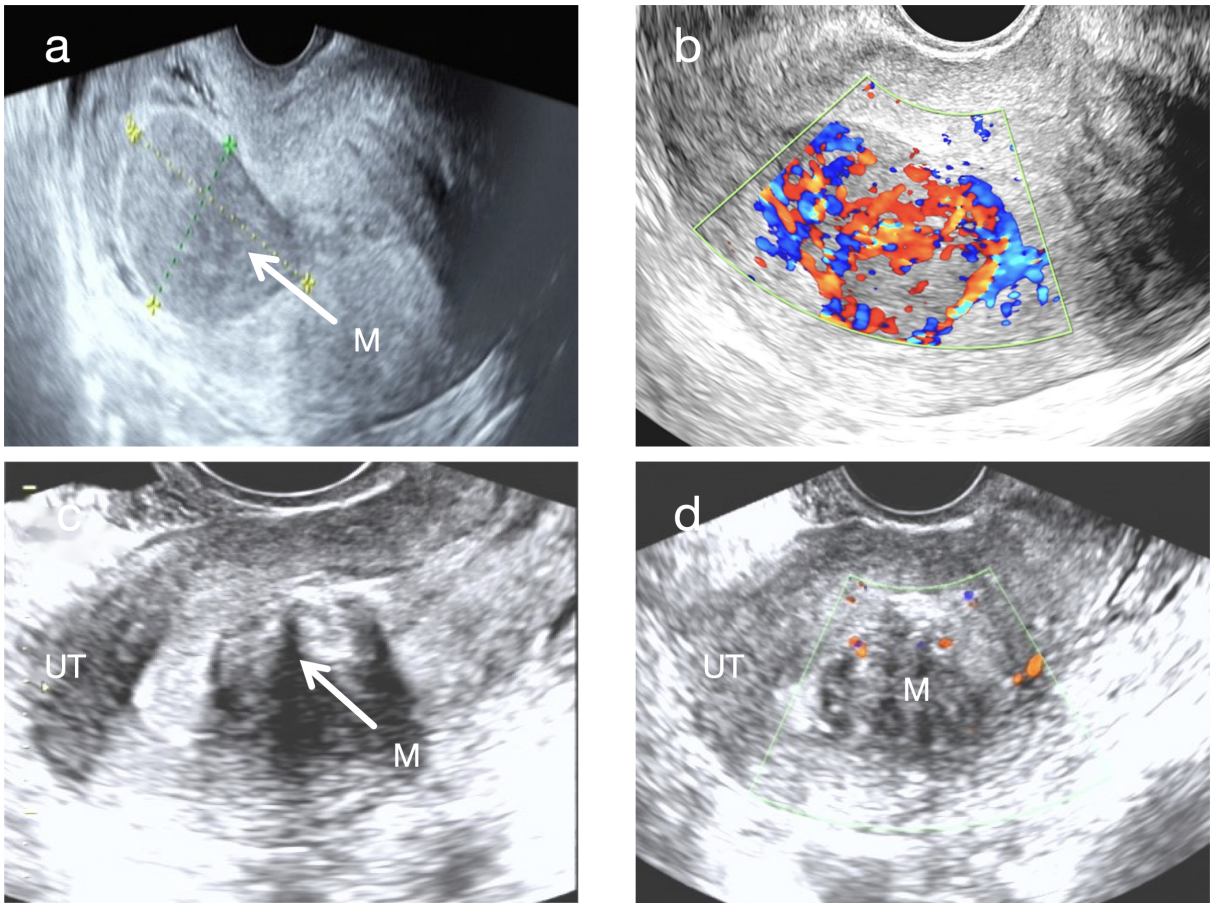

Fig. 2. Comparison of sonographic images between submucosal UIMT (Case 1) and typical submucosal uterine leiomyoma. (a) Sagittal ultrasonographic view of the submucosal UIMT mass. White arrows indicate the tumor masses. (b) CDFI showing abundant blood flow signals within the submucosal UIMT mass (Adler grade 3) with a "colorful mosaic sign". (c) Sagittal ultrasound view of a typical submucosal uterine leiomyoma. White arrows indicate the tumor masses. (d) CDFI showing sparse blood flow signals in the typical submucosal uterine leiomyoma (Adler grade 1).

raphy. Compared with typical uterine leiomyomas, UIMTs showed richer color Doppler flow signals (Fig. 2b,d). In particular, Cases 1 and 2 exhibited extremely abundant vascularity, forming a characteristic "colorful mosaic sign" (Fig. 1b, Fig. 2b).

A key observation in this study was the "blurred halo sign", identified as a typical ultrasonographic feature of UIMT. This sign is characterized by scattered strip-like or patchy hyperechoic areas within a hypoechoic background (Fig. 1a, Fig. 2a). It is clearly distinguishable from the "whorled pattern" typically observed in conventional leiomyomas (Fig. 2c). In leiomyomas, heterogeneous hypoechoic or isoechoic areas create whorled textures due to interwoven smooth muscle cells and connective tissue fibers. In contrast, UIMT lesions display more homogeneous, dense internal echoes. Its signal on magnetic resonance imaging (MRI) also appears relatively homogeneous (Fig. 1c), whereas leiomyomas generally show lower and more disorganized echogenicity (Fig. 2a,c). However, overlap in imaging features may occur when leiomyomas undergo degenerative changes, such as mixed echogenicity or cystic transformation [11]. In such instances, the diagnostic utility of the "blurred halo sign" when combined with abundant blood flow signals becomes even more prominent.

Although most UIMTs are benign, they can infiltrate adjacent tissues or recur postoperatively [12]. Therefore, when sonography reveals a large uterine mass with patchy hyperechoic areas, indistinct margins, and abundant blood flow, clinicians should maintain a high index of suspicion for UIMT to differentiate it from ordinary leiomyomas.

4.2 Significance of Clinical Features

UIMT can occur in women across different reproductive age groups [13,14]. In this study, the main clinical manifestations included prolonged menstrual periods, increased menstrual flow, and dysmenorrhea. This is consistent with the findings of Bai *et al*. (2024) [6], who reported that "abnormal uterine bleeding is the most common symptom of UIMT". The UIMT masses in this study

were generally large, with 2 located in the submucosa. Mechanical compression of the endometrium by the masses likely contributed to increased menstrual volume and prolonged menstrual periods. Fifty percent (3 cases) of patients had dysmenorrhea, possibly due to the release of local inflammatory mediators by the tumor [15]. This proportion is slightly higher than that reported by Bai *et al.* (2024) [6], which may be attributed to the smaller sample size. In terms of laboratory findings, all 6 patients presented varying degrees of anemia, possibly resulting from chronic blood loss secondary to prolonged or heavy menstruation. Case 4 exhibited elevated white blood cell counts, and Cases 2 and 3 showed both elevated CA125 and white blood cell levels, findings potentially linked to local inflammatory responses elicited by the tumor stimulating the immune system. This agrees with the conclusion by Bennett *et al.* (2017) [15] that "UIMT exhibits significant inflammatory infiltration characteristics". In this study, 2 patients (33.3%) had a history of thyroid disease—1 with hyperthyroidism and one with papillary thyroid carcinoma (postoperatively managed). This comorbidity may not be coincidental. Rodríguez-Castelán *et al.* (2019) [16] showed in rabbit models that hypothyroidism induces uterine hyperplasia and inflammation by altering sex hormone receptor expression—consistent with UIMT's core pathological features of myofibroblastic proliferation and inflammatory infiltration, sharing a common "hormonal regulation-tissue hyperplasia-inflammation" pathway. Shinderman-Maman *et al.* (2018) [17], though focusing on ovarian cancer, confirmed that thyroid hormones promote tumorigenesis through transcriptional regulation, offering a potentially translatable molecular mechanism underlying UIMT-thyroid associations. Notably, no studies have quantified their co-occurrence rate, and our limited sample size precludes causal inference. Future case-control studies with larger cohorts should measure thyroid hormone levels in UIMT patients (and correlate them with tumor size or invasiveness) and assess co-expression of thyroid-related and UIMT driver genes to clarify the underlying mechanisms. In conclusion, the clinical features of UIMT are nonspecific, and asymptomatic patients warrant active screening. Abnormal uterine bleeding and pelvic masses in women of childbearing age should be evaluated comprehensively.

4.3 Pathological Features

UIMT comprises differentiated myofibroblasts and abundant inflammatory infiltration, showing intermediate biological behavior with potential for recurrence and metastasis [18–20]. Approximately 50% of cases harbor *ALK* rearrangement, with 87.5%–100% *ALK* positivity [21–23]. Here, all 6 cases showed *ALK* gene break signals, supporting ALK's role in tumorigenesis and its diagnostic value as a key molecular marker [24]. Heterogeneous CD10 and H Caldesmon expression patterns further reflect molecular diversity; 2 cases had infiltrative growth into surrounding tissues, highlighting the tumor's non-negligible invasiveness.

According to the latest WHO classification, UIMT includes three histological subtypes: (1) Loosely arranged myofibroblasts with mucus, rich vessels, and inflammatory infiltration; (2) Densely packed spindle cells with mucus or collagen regions; and (3) Scar-like hyperplasia with scattered inflammatory cells. All 6 cases in this study presented features of the myxoid and dense spindle-cell types (Fig. 1d), with mild cellular atypia and abundant cytoplasm—features that can lead to misdiagnosis as uterine leiomyoma or spindle cell sarcoma [25,26]. Thus, accurate diagnosis requires an integrated assessment combining histopathology and immunohistochemistry, with ALK expression and rearrangement serving as key criteria.

4.4 Treatment Methods and Prognosis

All 6 patients underwent surgical treatment, and no recurrence or metastasis was observed during 21–57 months of follow-up. The surgical approach should be individualized based on tumor location, size, invasion depth, and the patient's fertility requirements. Recent studies indicate that minimally invasive techniques—such as laparoscopy and hysteroscopy—are preferred for UIMT. For patients desiring fertility preservation, careful monitoring and long-term follow-up are essential [27].

4.5 Research Limitations and Future Research Directions

This study has several limitations, including a small sample size, a retrospective design, and potential selection bias. As inflammatory myofibroblastic tumors are rare, current knowledge—derived mainly from short-term follow-up cases—remains limited. The application of contrast-enhanced ultrasound to assess lesion perfusion may enhance diagnostic accuracy.

Future studies should address the complexity of UIMT and patient heterogeneity (e.g., age, gender, genetic background). Integrating high-throughput sequencing and artificial intelligence (AI) to investigate the tumor microenvironment could elucidate the molecular mechanisms and genetic underpinnings of UIMT, thereby facilitating precision medicine, early diagnosis, and individualized treatment strategies [28].

5. Conclusions

UIMT is a rare borderline tumor characterized by typical sonographic features including a solid mass with heterogeneous echotexture ("blurred halo sign") and abundant color Doppler flow ("colorful mosaic sign"). Ultrasound effectively delineates the tumor's location, size, echotextural characteristics, and boundaries; moreover, it allows dynamic monitoring of lesion progression, making it an ideal tool for assessing disease evolution and postoperative recurrence. Given UIMT's potential for invasiveness, clinicians should maintain a high index of suspicion and include

it in the differential diagnosis. A deeper understanding of UIMT's sonographic and clinical features is crucial for improving diagnostic accuracy and patient prognosis.

Availability of Data and Materials

The datasets used and analyzed during the current study are available from the corresponding author upon reasonable request.

Author Contributions

YTM: Contributed to data collection and organization, data analysis, and writing and revision of the original manuscript; MHL: Participated in data collection and organization and manuscript review; KY: Participated in data collection and organization; XD: Participated in imaging data collection and organization; HYK: Participated in study design and conception, assisted in data organization, and participated in manuscript revision; YCL: Participated in study design and conception, assisted in data organization, and participated in manuscript revision; YL: were responsible for study design, original draft, supervision and review. All authors contributed to editorial changes in the manuscript. All authors read and approved the final manuscript. All authors have participated sufficiently in the work and agreed to be accountable for all aspects of the work.

Ethics Approval and Consent to Participate

The study was approved by the Ethics Committee of Hunan Provincial Maternal and Child Health Hospital in 2025 (ethical approval number: No.: JSKY-2025-11-002); Relevant information has been fully disclosed to the patients, and informed consent has been obtained. The study was carried out in accordance with the guidelines of the Declaration of Helsinki.

Acknowledgment

We would like to express our sincere gratitude to all individuals who contributed to the preparation of this manuscript.

Funding

(1) Hunan Provincial Science and Technology Innovation Program (2021SK50607). (2) Scientific Research Program of Hunan Provincial Health Commission (202209023037.00).

Conflict of Interest

The authors declare no conflict of interest.

References

[1] WHO Classification of Tumours Editorial Board. WHO Classification of Tumours: Soft Tissue and Bone Tumours. 5th edn. IARC Press: Lyon. 2020.

[2] Patnana M, Sevrukov AB, Elsayes KM, Viswanathan C, Lubner M, Menias CO. Inflammatory pseudotumor: the great mimicker. AJR. American Journal of Roentgenology. 2012; 198: W217–W227. https://doi.org/10.2214/AJR.11.7288.

[3] Sbaraglia M, Bellan E, Dei Tos AP. The 2020 WHO Classification of Soft Tissue Tumours: news and perspectives. Pathologica. 2021; 113: 70–84. https://doi.org/10.32074/1591-951X-213.

[4] Adler DD, Carson PL, Rubin JM, Quinn-Reid D. Doppler ultrasound color flow imaging in the study of breast cancer: preliminary findings. Ultrasound in Medicine & Biology. 1990; 16: 553–559. https://doi.org/10.1016/0301-5629(90)90020-d.

[5] Chinese Society of Gynecologic Oncology. Chinese Gynecologic Oncology Clinical Practice Guidelines 2024. People's Medical Publishing House: Beijing. 2024.

[6] Bai L, Han L, Zheng A, Chen Y. Uterine inflammatory myofibroblastic tumor: a retrospective analysis. Frontiers in Oncology. 2024; 14: 1461092. https://doi.org/10.3389/fonc.2024.1461092.

[7] Huang HJ, Chen XY, Zheng SL, Zhong DR. Clinicopathological and molecular genetic characteristics of 32 cases of uterine inflammatory myofibroblastic tumor. Chinese Journal of Clinical and Experimental Pathology. 2023; 39: 1207–1211. https://doi.org/10.13315/j.cnki.cjcep.2023.10.012. (In Chinese)

[8] Bhardwaj B, Guleria P, Tevatia A, Pethan M, Sharma S, Rana M. Inflammatory myofibroblastic tumour of cervix: Uncommon pathology in an unlikely location - A literature review. European Journal of Obstetrics & Gynecology and Reproductive Biology: X. 2025; 26: 100375. https://doi.org/10.1016/j.eurox.2025.100375.

[9] Yan XY, Liu YJ, Shao YM, Tan L, Xiao MS, Wei Y, *et al*. Ultrasonic characteristics of inflammatory myofibroblastic tumor. Chinese Journal of Ultrasound in Medicine. 2025; 41: 228–230. https://doi.org/10.3969/j.issn.1002-0101.2025.02.030. (In Chinese)

[10] Zhao LH, Zhou LL. Ultrasonic features of inflammatory myofibroblastic tumor in the female reproductive system. Chinese Journal of Ultrasound in Medicine. 2022; 38: 951–953. https://doi.org/10.3969/j.issn.1002-0101.2022.08.034. (In Chinese)

[11] Wang X. Ultrasonic characteristics and diagnostic strategies of uterine leiomyoma based on the practical work of ultrasound department in primary hospitals. Contemporary Medical Symposium. 2024; 22: 94–97. https://doi.org/10.3969/j.issn.2095-7629.2024.36.028. (In Chinese)

[12] Etlinger P, Kuthi L, Kovács T. Inflammatory Myofibroblastic Tumors in the Uterus: Childhood-Case Report and Review of the Literature. Frontiers in Pediatrics. 2020; 8: 36. https://doi.org/10.3389/fped.2020.00036.

[13] Karpathiou G, Devouassoux-Shisheboran M, Stolnicu S, Chauleur C, Péoc'h M. Uterine inflammatory myofibroblastic tumor. Pathology, Research and Practice. 2023; 242: 154335. https://doi.org/10.1016/j.prp.2023.154335.

[14] Shukla PS, Mittal K. Inflammatory Myofibroblastic Tumor in Female Genital Tract. Archives of Pathology & Laboratory Medicine. 2019; 143: 122–129. https://doi.org/10.5858/arpa.2017-0575-RA.

[15] Bennett JA, Nardi V, Rouzbahman M, Morales-Oyarvide V, Nielsen GP, Oliva E. Inflammatory myofibroblastic tumor of the uterus: a clinicopathological, immunohistochemical, and molecular analysis of 13 cases highlighting their broad morphologic spectrum. Modern Pathology: an Official Journal of the United States and Canadian Academy of Pathology, Inc. 2017; 30: 1489–1503. https://doi.org/10.1038/modpathol.2017.69.

[16] Rodríguez-Castelán J, Del Moral-Morales A, Piña-Medina AG, Zepeda-Pérez D, Castillo-Romano M, Méndez-Tepepa M, *et al*. Hypothyroidism induces uterine hyperplasia and inflammation related to sex hormone receptors expression in virgin rabbits.

Life Sciences. 2019; 230: 111–120. https://doi.org/10.1016/j.lfs.2019.05.063.

[17] Shinderman-Maman E, Weingarten C, Moskovich D, Werner H, Hercbergs A, Davis PJ, *et al*. Molecular insights into the transcriptional regulatory role of thyroid hormones in ovarian cancer. Molecular Carcinogenesis. 2018; 57: 97–105. https://doi.org/10.1002/mc.22735.

[18] Fletcher CD, Unnik K, Mertens F (eds.) Pathology and genetics of tumors of soft tissue and bone (pp. 91–95). IARC Press: Lyon. 2002.

[19] Khatri A, Agrawal A, Sikachi RR, Mehta D, Sahni S, Meena N. Inflammatory myofibroblastic tumor of the lung. Advances in Respiratory Medicine. 2018; 86: 27–35. https://doi.org/10.5603/ARM.2018.0007.

[20] WHO Classification of Tumours Editorial Board. WHO Classification of Tumours: Female Genital Tumours (pp. 298–299). 5th ed. IARC Press: Lyon. 2020.

[21] Zhang Y, Dong W, Li SX, Zhao JJ, Du B. Clinical and molecular pathological features of uterine inflammatory myofibroblastic tumor. Zhonghua Bing Li Xue Za Zhi = Chinese Journal of Pathology. 2021; 50: 1020–1023. https://doi.org/10.3760/cma.j.cn112151-20210110-00024. (In Chinese)

[22] Preobrazhenskaya EV, Iyevleva AG, Suleymanova AM, Tiurin VI, Mitiushkina NV, Bizin IV, *et al*. Gene rearrangements in consecutive series of pediatric inflammatory myofibroblastic tumors. Pediatric Blood & Cancer. 2020; 67: e28220. https://doi.org/10.1002/pbc.28220.

[23] Kuisma H, Jokinen V, Pasanen A, Heikinheimo O, Karhu A, Välimäki N, *et al*. Histopathologic and Molecular Characterization of Uterine Leiomyoma-like Inflammatory Myofibroblastic Tumor: Comparison to Molecular Subtypes of Uterine Leiomyoma. The American Journal of Surgical Pathology. 2022; 46: 1126–1136. https://doi.org/10.1097/PAS.0000000000001904.

[24] Mohammad N, Haimes JD, Mishkin S, Kudlow BA, Leong MY, Chew SH, *et al*. ALK Is a Specific Diagnostic Marker for Inflammatory Myofibroblastic Tumor of the Uterus. The American Journal of Surgical Pathology. 2018; 42: 1353–1359. https://doi.org/10.1097/PAS.0000000000001120.

[25] Hu GM, Chen HP, Zhang RZ, Wu HF. Clinicopathological analysis of 2 cases of uterine spindle cell sarcoma with NTRK rearrangement. Chinese Journal of Pathology. 2024; 53: 480–482. https://doi.org/10.3760/cma.j.cn112151-20230920-00194. (In Chinese)

[26] Li XQ, Hisaoka M, Shi DR, Zhu XZ, Hashimoto H. Expression of anaplastic lymphoma kinase in soft tissue tumors: an immunohistochemical and molecular study of 249 cases. Human Pathology. 2004; 35: 711–721. https://doi.org/10.1016/j.humpath.2003.12.004.

[27] Mandato VD, Valli R, Mastrofilippo V, Bisagni A, Aguzzoli L, La Sala GB. Uterine inflammatory myofibroblastic tumor: more common than expected: Case report and review. Medicine. 2017; 96: e8974. https://doi.org/10.1097/MD.0000000000008974.

[28] Xu H, Cong F, Hwang TH. Machine Learning and Artificial Intelligence-driven Spatial Analysis of the Tumor Immune Microenvironment in Pathology Slides. European Urology Focus. 2021; 7: 706–709. https://doi.org/10.1016/j.euf.2021.07.006.